OMTO, Volume *25*

Supplemental information

miR-15a and miR-15b modulate natural killer and $CD8^+$T-cell activation and anti-tumor immune response by targeting PD-L1 in neuroblastoma

Anup S. Pathania, Philip Prathipati, Omalla A. Olwenyi, Srinivas Chava, Oghenetejiri V. Smith, Subash C. Gupta, Nagendra K. Chaturvedi, Siddappa N. Byrareddy, Don W. Coulter, and Kishore B. Challagundla

Supplementary Figure 1

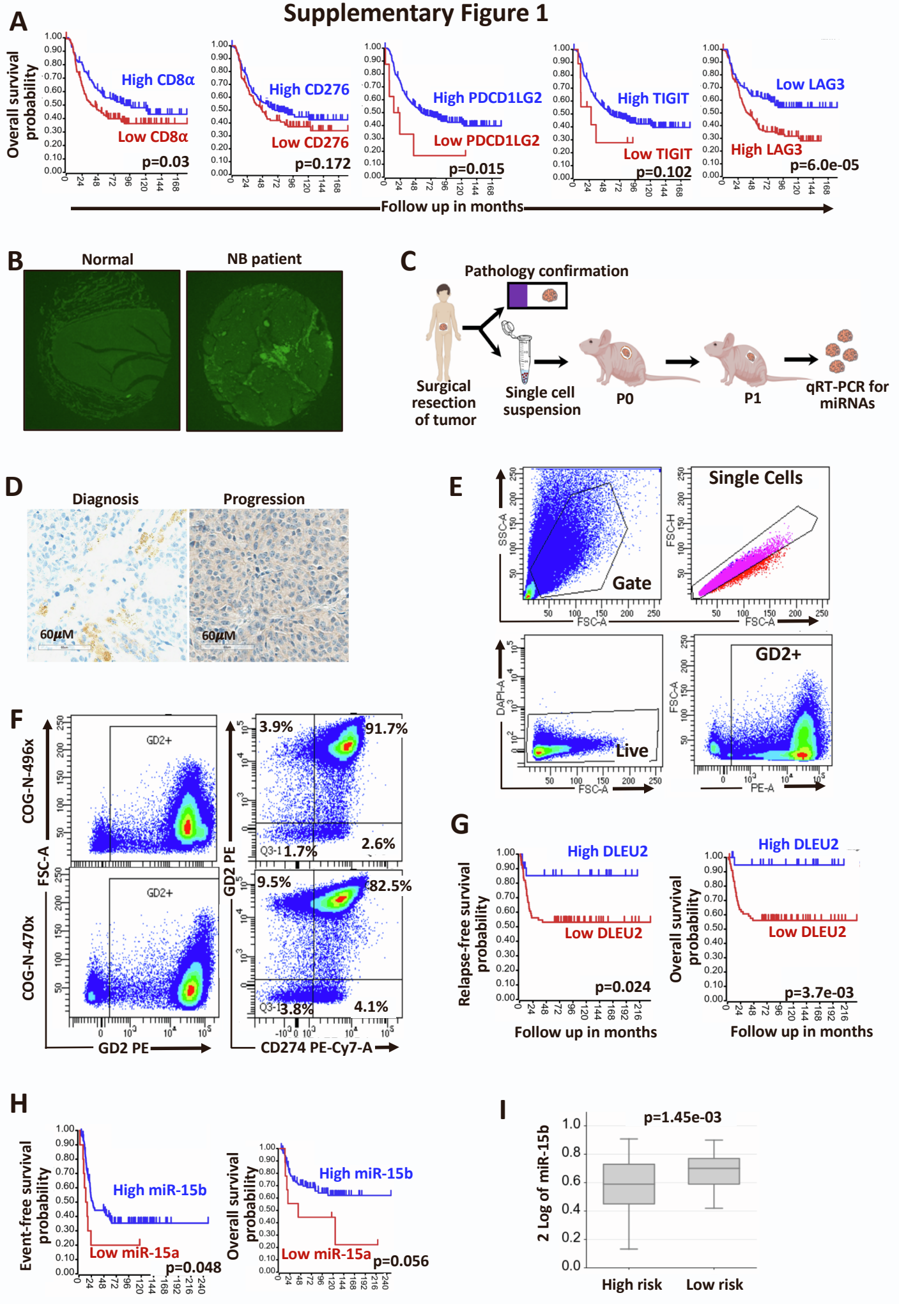

Supplementary Figure 1.

(A) Kaplan-Meier curves showing event-free and overall survival probability rates with different levels of CD8α, CD276, PDCD1LG2, TIGIT and LAG-3 in NB patients from the TARGET dataset. (B) Immunofluorescence images of PD-L1 on NB patient tumor and normal tissue microarrays photographed at 5X. (C) A schematic model displaying the procedure for establishing NB PDX tumor generation, implantation, and expansion in nude mice. The surgical procedure removed tumor tissues from patients, followed by single-cell preparation and subcutaneous injection into mice. Tumor tissues were harvested once the tumor reached end volume, then prepared a single-cell suspension, and ready for re-implantation in the next set of mice in multiple passages for expansion and was used for the experiments. P0 = Passage 0, P1 = Passage 1. (D) A representative IHC staining of total PD-L1 in NB PDX tumors of NB patients at the diagnosis and progression stages. (E) The gating strategy of GD2 enriched PDX-derived tumor cell population achieved through cell sorting by flow cytometry using PE-GD2 antibodies. (F) Representative flow cytometric plots showing the surface expression of PD-L1 on $GD2^{+ve}$ NB tumor cells isolated freshly from PDX tumor tissues. Percentage $PD\text{-}L1^{+ve}$ cells are shown in each quadrant. (G) Kaplan-Meier curves showing overall and relapse-free survival probability rates with different levels of the miR-15a host gene, *DLEU2* in the 88 NB patient samples in the Versteeg (GSE16476) dataset. (H) Kaplan-Meier curves showing overall and event-free survival probability rates with different levels of the miR-15b in NB patients (n=139) from the Tumor NB ALT-Westermann−144-tpm-gencode19 R2 dataset. (I) Box plots showing the expression of miR-15B in high-risk vs low-risk NB patient samples (n=96, GSE73515).

Supplementary Figure 2

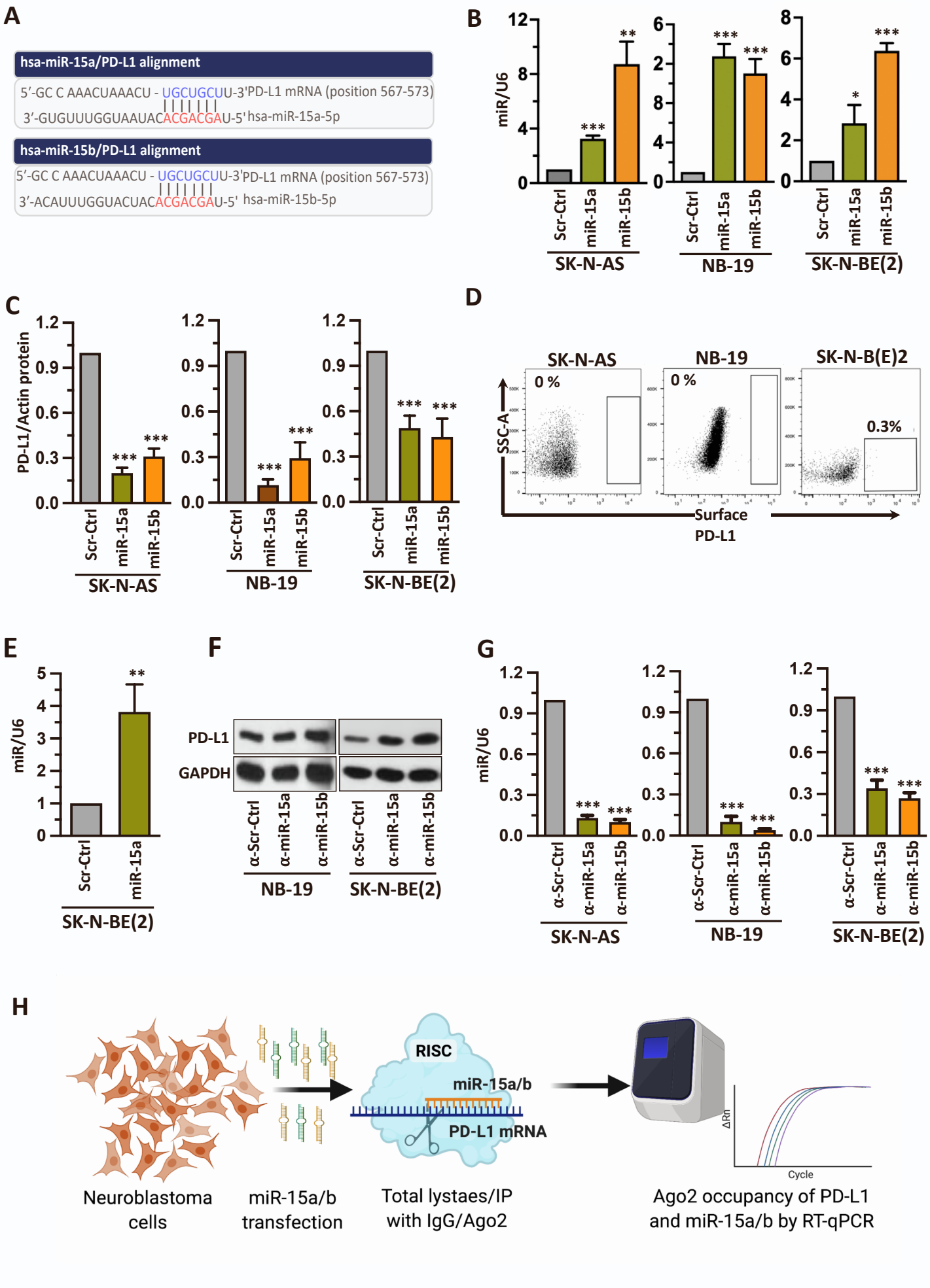

Supplementary Figure 2.
(A) The sequence alignment shows the predicted binding sites between miR-15a, miR-15b, and 3'UTR of PD-L1 mRNA. Complementary sequences of PD-L1 mRNA and miRNAs are shown in blue and red, respectively. (B) Representative quantification graphs showing miR-15a and miR-15b levels normalized to U6 in NB cells transfected with miR-15a, miR-15b, or Scr Ctrl oligonucleotides for 48 h. (C) Representative quantification graphs showing total PD-L1 normalized to actin in NB cells transfected with miR-15a, miR-15b, or Scr Ctrl oligonucleotides for 48 h. (D) Representative flow cytometric plots showing a FMO control of cells stained with all fluorochromes except one used to set the background signal for PD-L1 in SK-N-AS (left panel), NB-19 (middle panel), and SK-N-B(E)2 (right panel) cells. A tube containing an unstained negative control or beads was used as compensation controls. (E) Representative quantification graph showing miR-15a levels normalized to U6 in SK-N-BE(2) cells stably expressing miR-15a for 48 h. (F) Western blotting for PD-L1 total protein in NB cells transfected with inhibitors of miRs such as α-miR-15a, α-miR-15b or α- Scr Ctrl oligonucleotides for 48h. (G) Representative quantification graph showing miR-15a and miR-15b levels normalized to U6 in NB cells transfected with inhibitors of miRs such as α-miR-15a, α-miR-15b or α- Scr Ctrl oligonucleotides for 48h. (H) A schematic representation of the Ago2 immunoprecipitation (IP) experiment to identify Ago2 occupied PD-L1 mRNA, miR-15a, and miR-15b in NB cells. Data represent mean ± standard error of 3-4 independent biological experiments. Statistical analyses were performed using a two-sided unpaired *t*-test. ***$p < 0.001$, **$p < 0.01$.

Supplementary Figure 3

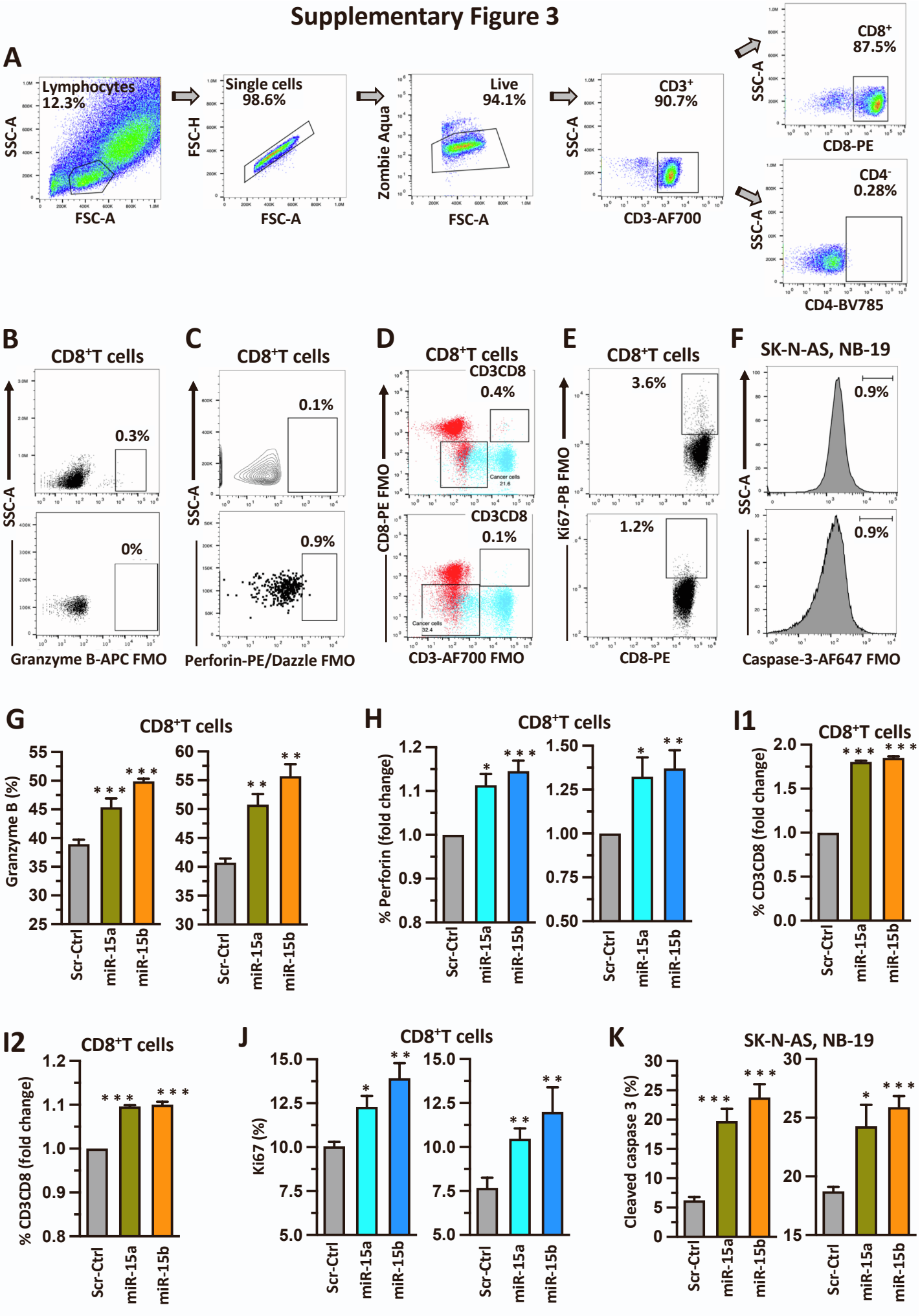

Supplementary Figure 3.

(A) Representative flow cytometric pseudo color plots showing the gating strategy used to isolate human $CD8^+$T cells. Untouched $CD8^+$T cells were isolated from PBMCs of healthy human blood donors by negative selection using the MojoSort™ human $CD8^+$T Cell Isolation Kit. The dead cells were identified and excluded from the final analysis by gating on the Zombie Aqua™ viability dye negative population, live cells. Cells were fluorescently stained with CD3-AF700, CD8-PE, CD4-BV785, and $CD3^+CD8^+CD4^-$ cells were used in the study. (B-F) Representative flow cytometric plots were showing *a* FMO control of cells stained with all fluorochromes except one used to set the background signal for Granzyme B^+ (B), $Perforin^+$ (C), $CD3^+/CD8^+$ (D), Ki-67^+ (E) and cleaved caspase-3 (F) in experiments of Figure.3. A tube containing an unstained negative control or beads was used as compensation controls. (G-J) Bar graphs showing flow cytometric quantitative analysis of Granzyme B (G), Perforin (H), CD3/CD8 (I1,2), and Ki-67^+ (J) in $CD8^+$T cells cocultured with miR-15a and miR-15b expressing SK-N-AS (G-J, left panels), and NB-19 (G-J, right panels) cells. (K) A representative flow cytometric quantitative analysis of intracellular active caspase-3 in miR-15a and miR-15b expressing SK-N-AS (left panel) and NB-19 (right panel) cells upon coculture with activated human $CD8^+$T Cells (E:T ratio=1:1) for 48 h. Data represent mean ± standard error of 3-5 independent biological experiments. Statistical analyses were performed using a two-sided unpaired *t*-test. *$p< 0.05$, **$p< 0.01$, ***$p< 0.001$.

Supplementary Figure 4

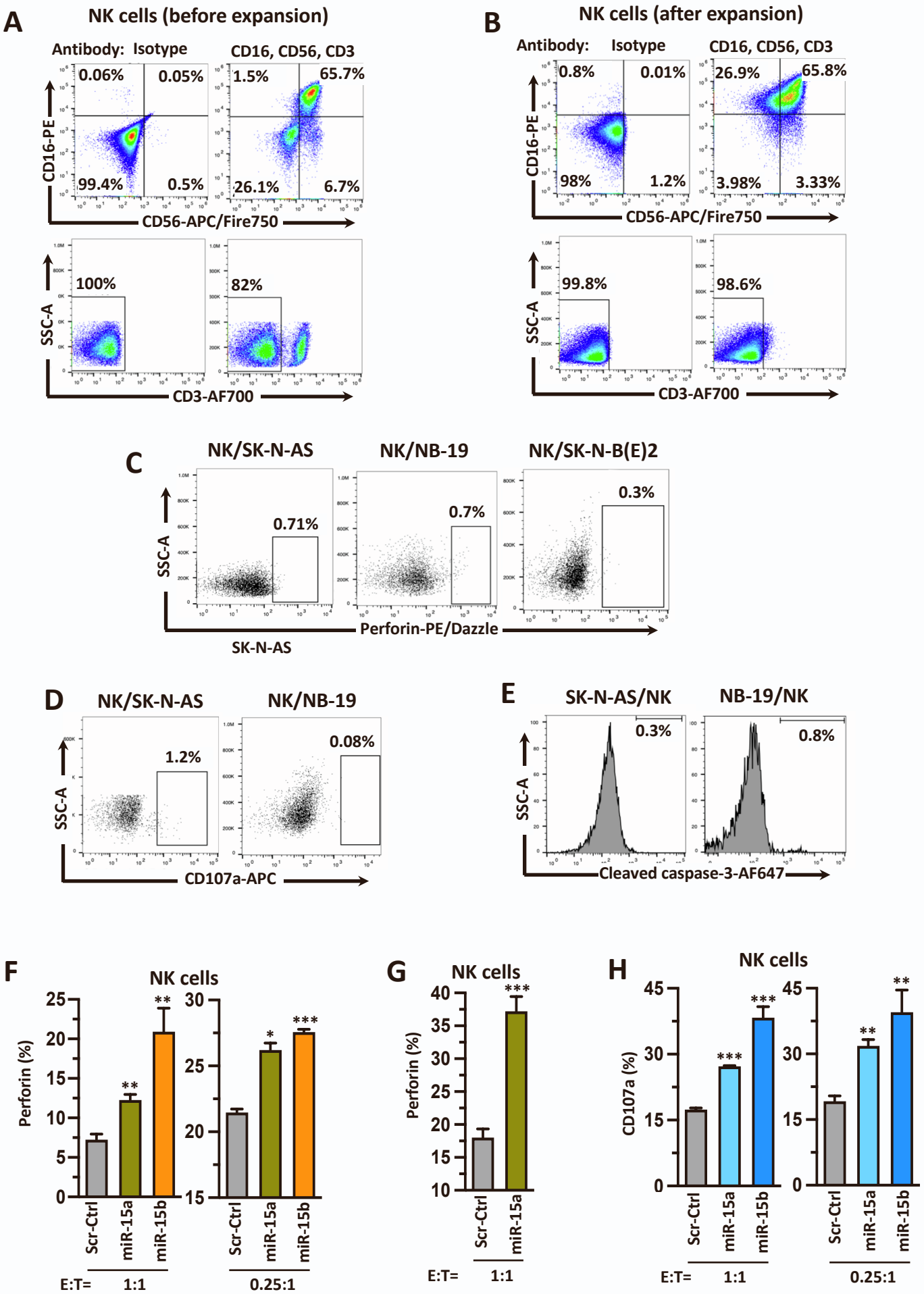

Supplementary Figure 4 continued

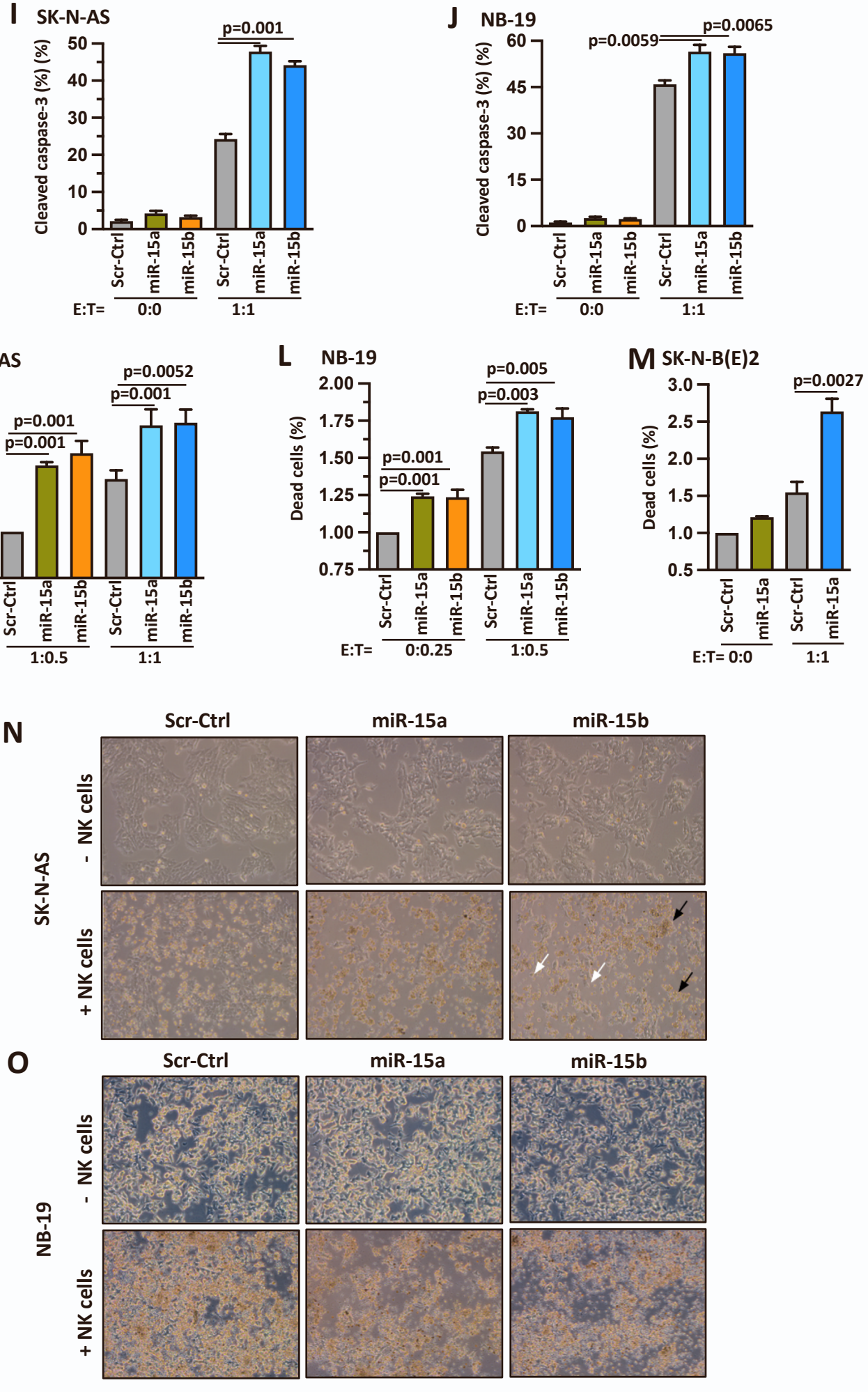

Supplementary Figure 4.

(A,B) Representative flow cytometric pseudocolor plots showing human NK cells purity before and after expansion *ex vivo* using irradiated K562-mbIL21 feeder cells and IL-2 for 14 days. NK cells were fluorescently stained with CD3-AF700, CD56-APC/Fire750, CD16-PE, and $CD3^{-}CD56^{+}CD16^{+}$ cells were used in the study. (C-E) Representative flow cytometric plots showing a FMO *control* of cells stained with all fluorochromes except one used to set the background signal for perforin (C), CD107a (D), and cleaved caspase-3 in experiments of Figure.4. A tube containing an unstained negative control or beads was used as compensation controls. (F-H) A representative flow cytometric quantitative analysis of perforin (F,G), CD107a (H) in NK cells after coculture with miR-15a or miR-15b expressing SK-N-AS (F,H left panels), stable miR-15a expressing SK-N-B(E)2 (G), and NB-19 (F,H right panels) cells 5 h. A representative flow cytometric quantitative analysis of intracellular cleaved caspase-3 (I,J), and dead cells (K-M) in miR-15a or miR-15b expressing SK-N-AS (I,K), NB-19 (J,L), and stable miR-15a expressing SK-N-B(E)2 (M) cells upon coculture (1:1 for SK-N-AS, 0.25:1 for NB-19 and 1:1 for SK-N-BE(2)) with activated human NK cells for 5h. (N,O) Phase-contrast microscope images of dead miR-15a and miR-15b expressing SK-N-AS (N), and NB-19 (O) cells upon coculture (E:T=1:1) with or without activated NK cells for 5h. The white arrow represents dying NB cells whereas the black arrow represents activated NK cells in action. Data represent mean ± standard error of 3-5 independent biological experiments. Statistical analyses were performed using a two-sided unpaired *t*-test. *$p< 0.05$, **$p< 0.01$, ***$p< 0.001$.

Supplementary Figure 5

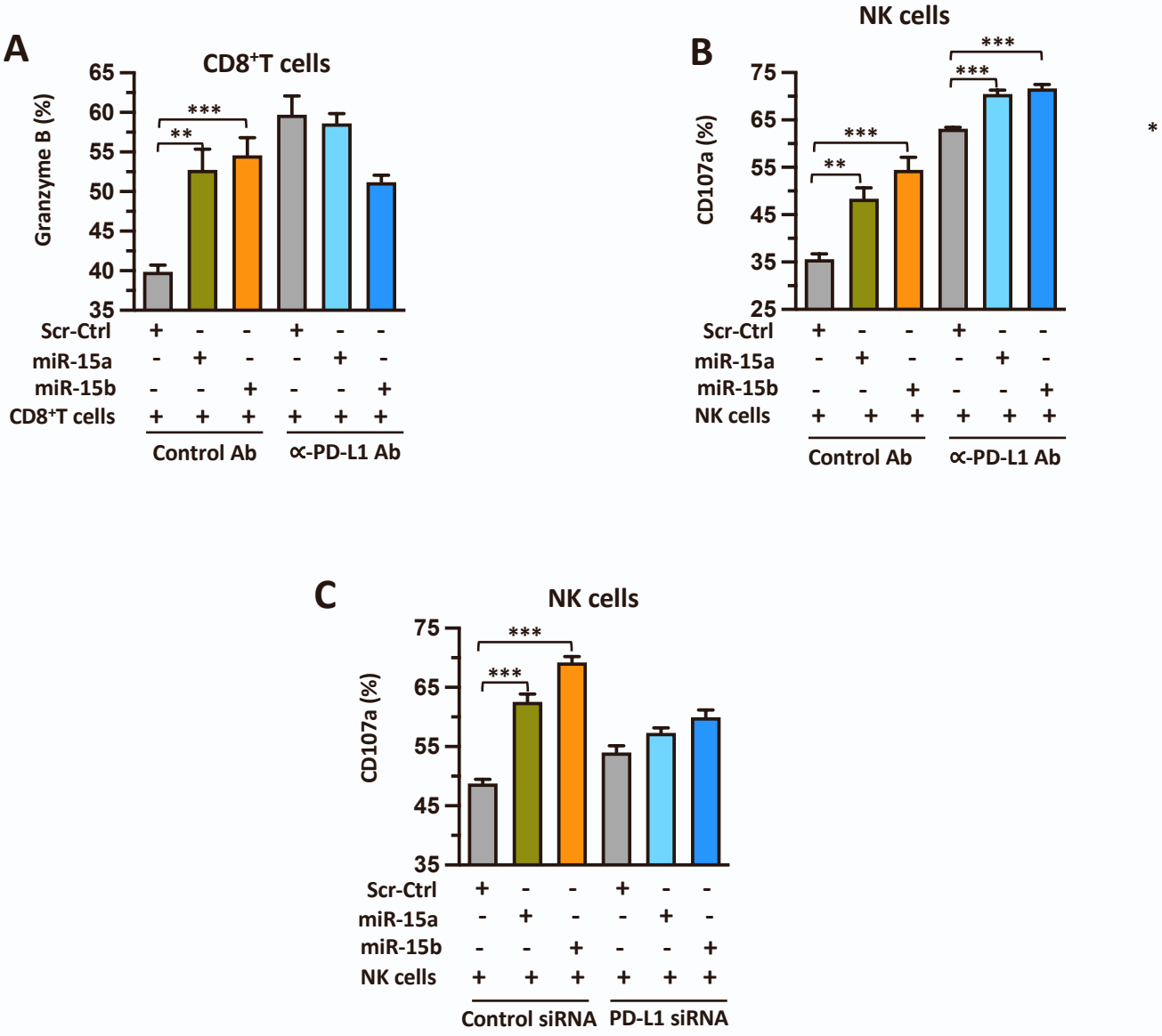

Supplementary Figure 5.
(A-C) Representative flow cytometric quantification graphs showing the expression of intracellular granzyme B (A) and surface CD107a (B,C) in $CD8^+$T (A) and NK cells (B,C) cocultured with miR-15a or miR-15b expressing SK-N-AS (A) cells blocked by treatment with anti-PD-L1 antibody for 24h (A,B) or treatment with PD-L1 siRNA for 24h (C). Data represent mean ± standard error of 3-5 independent biological experiments. Statistical analyses were performed using a two-sided unpaired *t*-test. **p< 0.01, ***p< 0.001.

Supplementary Figure 6

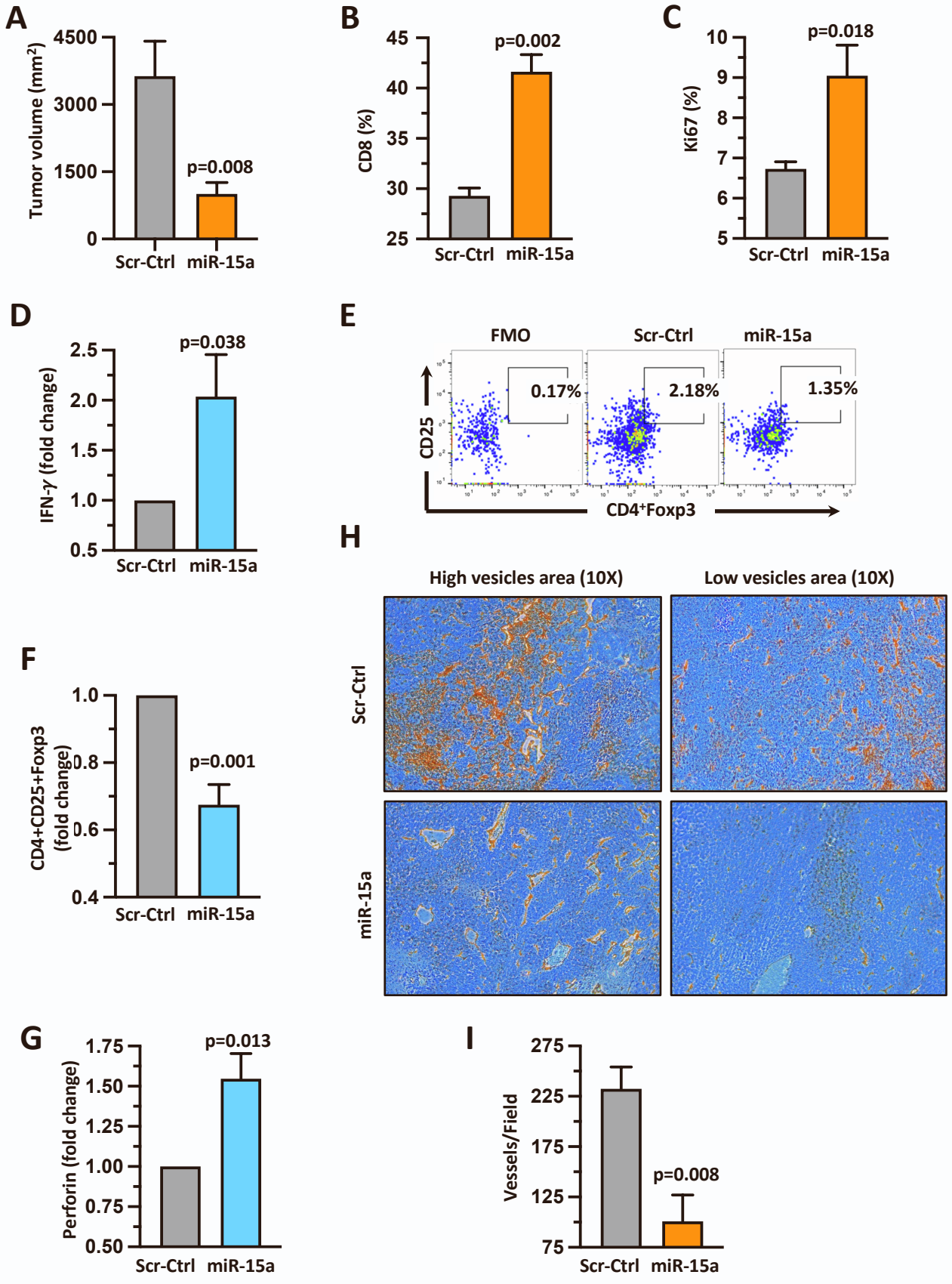

Supplementary Figure 6.
(A) Summary graph showing tumor volume of the C57BL/6 mice that received subcutaneous murine NB-975 cells stably expressing miR-15a or Scr ctrl miRNAs. (B-G) Representative flow cytometric plots/quantitative analysis graphs showing the percentage of CD8 cells, Ki-67, IFN-γ positive $CD8^+$T cells, Tregs and their quantification, and perforin positive mouse NK cells analyzed from the single-cell suspension of tumor tissues from C57BL/6 mice that received subcutaneous murine NB-975 cells stably expressing miR-15a or Scr ctrl miRNAs for 30 days. Tumor tissues were harvested, prepared as single-cell suspensions, gated on $CD4^+$ ($CD4^+CD25^+Foxp3^+$) population (α-mouse BV785-CD4, α-mouse PB-CD25, α-mouse/rat/human AF647- Foxp3) and stained for Tregs by flow cytometry using their respective antibodies. Representative flow cytometric plot showing a FMO control of cells stained with all fluorochromes except one used to set the background signal for the analysis was given. Bar graphs are shown as mean ± standard error (n=4 mice per group). (H,I) the representative IHC images of CD34 stained (murine endothelial cells) microvessels at 10X magnification and their quantification of mice tumors.